

Microcanonical-ensemble computer simulation of the high-temperature expansion coefficients of the Helmholtz free-energy of a Square-well fluid

Francisco Sastre,^{1,*} Elizabeth Moreno-Hilario,^{2,†} Maria
Guadalupe Sotelo-Serna,^{2,‡} and Alejandro Gil-Villegas^{1,§}

¹*Departamento de Ingeniería Física,
División de Ciencias e Ingenierías,
Campus León de la Universidad de Guanajuato*

²*División de Ciencias e Ingenierías,
Campus León de la Universidad de Guanajuato*

(Dated: June 25, 2018)

Abstract

The Microcanonical Ensemble computer simulation method (MCE) is used to evaluate the perturbation terms A_i of the Helmholtz free energy of a Square-Well (SW) fluid. The MCE method offers a very efficient and accurate procedure for the determination of perturbation terms of discrete-potential systems such as the SW fluid and surpass the standard NVT Canonical Ensemble Monte Carlo method, allowing the calculation of the first six expansion terms. Results are presented for the case of a SW potential with attractive ranges $1.1 \leq \lambda \leq 1.8$. Using semiempirical representation of the MCE values for A_i , we also discuss the accuracy in the determination of the phase diagram of this system.

Keywords: Microcanonical ensemble, discrete potentials, numerical simulations

*Electronic address: sastre@fisica.ugto.mx

†Electronic address: morenohe2013@licifug.ugto.mx

‡Electronic address: sotelosm2013@licifug.ugto.mx

§Electronic address: gil@fisica.ugto.mx

I. INTRODUCTION

Discrete potential (DP) systems have been investigated over the years in order to model properties of real substances, and offer a general and useful approach to represent properties of model systems interacting via continuous potentials [1]-[11]. The discretization process is based on the square-well (SW) fluid system, that becomes the basic input to describe more general discrete potentials and their mixtures. Examples of applications of DP systems to model real fluids have been biodiesel blends [12, 13] and two-dimensional equations of state for adsorption isotherms of noble gases [14], asphaltenes confined in porous materials [15], as well as carbon dioxide, hydrogen, water and methanol adsorbed onto carbon-based substrates [16–18].

The SW pair potential for spherical particles of diameter σ separated by a distance r is given by

$$\phi(r) = \begin{cases} \infty & \text{if } r \leq \sigma \\ \epsilon & \text{if } \sigma < r \leq \lambda\sigma \\ 0 & \text{if } r > \lambda\sigma \end{cases}, \quad (1)$$

where ϵ is the depth-well energy and λ is the range of the attractive interaction.

This system has been studied in great detail since it is a simple but at the same time complete model in order to understand the effect of non-conformal changes in the phase diagram and the dependence of the phase stability on the range of the attractive forces [19]-[31]. At the same time, it has been a key model for assessing the role played by multipolar moments when they are explicitly taken into account in the thermodynamic modeling of DP systems [32]-[36]. Thermodynamic and structural properties of the SW system have been fully determined over the years through computer simulations, thermodynamic perturbation methods and integral equation theories [37]-[51]. The combined use of these results has allowed to obtain accurate equations of state valid for the whole range of the fluid phase diagram, and in this way the SW system has become a key ingredient on robust approaches, such as the SAFT-VR method, to model a great variety of three and two-dimensional chain and branched molecular systems [25–27, 52, 53], including the description of lamellar phases [54]. Besides the SAFT models, alternative approaches to model anisotropic systems have taken into account the non-spherical shape of the molecules combined with a SW interaction [55]-[60]. More recently, it has been possible to generate accurate quantum thermodynamic

perturbation theories based on the SW model [61, 62].

In spite of these advances in the characterization of the SW system, and consequently in the improvement on the accuracy of equations of state for DP fluids, there are still challenges to assume. For example, the caloric properties as given by heat capacities and adsorption heats, require a better description of higher order perturbation terms. Following the Zwanzig's high-temperature perturbation expansion (HTE) [63], the excess Helmholtz free energy for a SW fluid can be expressed as a series on powers of the inverse thermal energy $\beta = 1/kT$,

$$\frac{A^E}{NkT} = \frac{A_0^E}{NkT} + \sum_{n=1}^{\infty} \beta^n A_n, \quad (2)$$

where A_n are the perturbation terms given by [38]

$$A_n = \lim_{\beta \rightarrow 0} \frac{1}{n!} \frac{\partial^n (A/NkT)}{\partial \beta^n} \quad (3)$$

and A_0^E is the hard-spheres (HS) Helmholtz free energy. The standard method to obtain exact values of the perturbation terms is through NVT-ensemble Monte Carlo simulations [38], where the perturbation terms are given as statistical averages of the attractive energy and their fluctuations, obtained from HS configurations. Recently, the Microcanonical computer simulation method (MCE) [64] was proposed as a straightforward approach to simulate thermodynamic properties of the SW fluid. Since in this ensemble the inverse thermal energy β is given in terms of the internal energy, it is possible to have a direct determination of the perturbation terms A_n according to the Zwanzig expansion. As we will discuss here, the MCE method can be used to accurately obtain HTE coefficients of order as higher as six, a task difficult to accomplish using the standard NVC ensemble MC method. The description of the method is given in Section II and its application to the case of the SW potential is presented in Section III, where parametric expressions for A_n are given in order to generate an equation of state, that is used for the evaluation of internal energies and isochoric heat capacities. Finally, in Section IV the main conclusions of this work are given.

II. SIMULATION METHOD

We describe briefly the simulation MCE method applied to fluids, that has been presented in our previous work [64], where the reader can found more details. This method

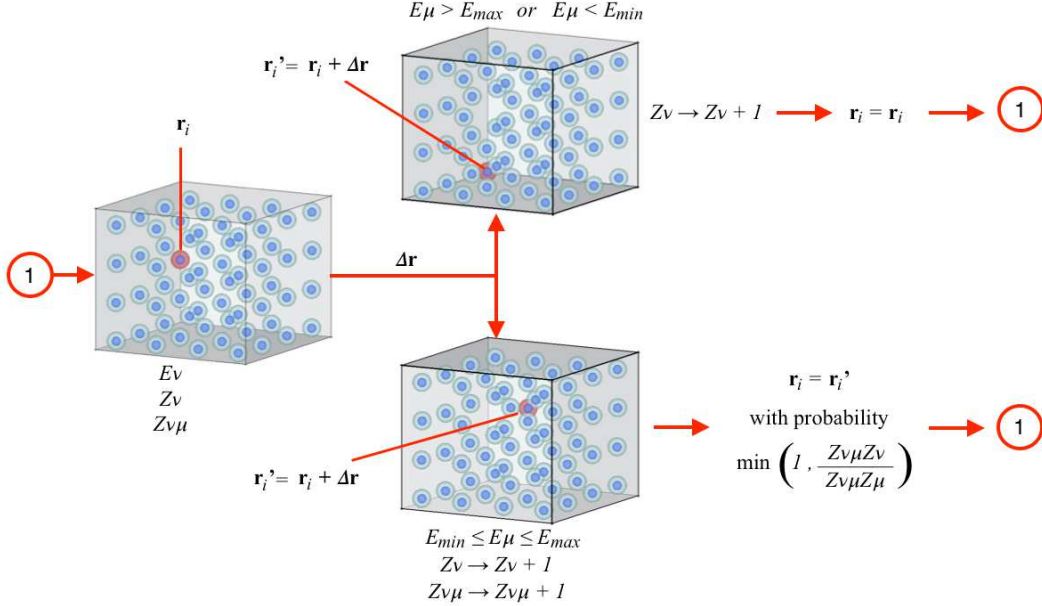


FIG. 1: (Color on line) Schematic representation of the Microcanonical Ensemble computer simulation method.

was originally developed for the computer simulation of the Ising model using a cluster algorithm [65] that optimizes a Broad Histogram Method [66]-[69]. Since the SW fluid has a discrete set of energy values as in the Ising model, the cluster algorithm is easily transferable to the SW fluid.

We consider a system of N spherical particles of diameter σ contained in a volume V that interact via the SW pair potential given by Eq.(1). The system can be characterized by its available energy levels E_ν , that are multiples of ϵ ,

$$E_\nu = -\nu\epsilon = \sum_{k,l \neq k} \phi(r_{kl}), \quad (4)$$

where r_{kl} is the distance between the centers of the k and l particles and ν is the number of particles pair that satisfies $\sigma < r_{kl} \leq \lambda\sigma$. The number of microstates that share the same energy E_ν is denoted by $\Omega(E_\nu)$. When a particle in a given microstate is displaced by $\Delta\mathbf{r}$, a new microstate is generated. After the displacement is applied to all N particles for each $\Omega(E_\nu)$ microstates, then $N\Omega(E_\nu)$ new microstates are created and just a given number of them, denoted by $V_{\nu\mu}$, will have energy E_μ . By the condition of reversibility, $V_{\nu\mu} = V_{\mu\nu}$ [68]. Two different protocols of allowed moves are used, based on either reversibility or

equiprobability. Thus if there is a random selection of one of the $\Omega(E_\nu)$ microstates with energy E_ν and a particle that is displaced by $\Delta\mathbf{r}$, then the probability that the system reaches the energy E_μ will be given as

$$P(E_\nu \rightarrow E_\mu) = \frac{V_{\nu\mu}}{N\Omega(E_\nu)}, \quad (5)$$

and for the reversal case

$$P(E_\mu \rightarrow E_\nu) = \frac{V_{\mu\nu}}{N\Omega(E_\mu)}. \quad (6)$$

In the simulation these probabilities are obtained by calculating the rate of attempts $T_{\nu\mu}$ to go from level ν to level μ . This can be achieved with two quantities:

- The number of times that the system spends in level ν , denoted by z_ν .
- The number of times that the system attempts to go from level ν to level μ , denoted by $z_{\nu\mu}$.

The values z_ν and $z_{\nu\mu}$ are obtained as follows:

1. With ν as the initial state, a particle is randomly chosen and z_ν is **always** incremented by 1.
2. Then a new energy E_μ is evaluated if a random displacement is applied to the chosen particle.
3. If E_μ is an allowed energy level, then $z_{\nu\mu}$ is **always** incremented by 1, independently of the acceptance of the particle displacement. It is possible to restrict the energy levels by discarding all cases where $E_\mu < E_{min}$ or $E_\mu > E_{max}$.
4. The particle displacement is accepted if $T_{\nu\mu} < T_{\mu\nu}$, otherwise the displacement is chosen with a probability equal to $T_{\mu\nu}/T_{\nu\mu}$.

The last condition assures that all levels are visited with equal probability, independently of their degeneracy. The initial values for z_i and $z_{\nu\mu}$ can be any positive number and after a large number of particle displacement attempts it will be observed that

$$\frac{z_{\nu\mu}}{z_\nu} \rightarrow T_{\nu\mu}, \quad (7)$$

and consequently

$$\frac{T_{\nu\mu}}{T_{\mu\nu}} = \frac{\Omega(E_\mu)}{\Omega(E_\nu)}. \quad (8)$$

This algorithm is highly efficient for evaluating the ratios $\Omega(E_\nu)/\Omega(E_\mu)$, or the differences $S_\nu - S_\mu$, using the microcanonical ensemble relation $S(E) = k \ln [\Omega(E)]$, because the number of times that the random number generator is required during the simulation is smaller than for NVT simulations. The efficiency increases if the number of allowed levels $(E_{max} - E_{min})/\epsilon$ is decreased. The entropy can be expressed as

$$S(E_\mu) = S(E_\nu) + \epsilon\eta\beta(E_\nu) + \dots, \quad (9)$$

where $\beta(E) = \partial S/\partial E$ is the inverse thermal energy, and η is an integer such that $E_\mu = E_\nu + \eta\epsilon$. The rest of the terms can be discarded, as long as N is large enough, and then we have

$$\ln(T_{\nu\mu}/T_{\mu\nu}) \approx \frac{\epsilon\eta}{k} \left. \frac{\partial S}{\partial E} \right|_\nu. \quad (10)$$

The last equation allow us to evaluate the inverse thermal energy as function of the internal energy [64],

$$\beta(E_\nu) = \frac{1}{6} \sum_{\eta=-3}^3 \frac{1}{\eta} \ln(T_{\nu,\nu+\eta}/T_{\nu+\eta,\nu}), \quad \eta \neq 0, \quad (11)$$

as well as the isochoric heat capacity $c(E)$,

$$c(E) = -\frac{[\beta(E)]^2}{S''}, \quad (12)$$

where $S'' = \partial^2 S/\partial E^2$. In Figure 1 we summarize the MCE method.

The very relevant feature of the MCE method to determine the HTE coefficients A_n is given by the fact that when the entropy is maximum, the curves $\beta(E)$ can be accurately evaluated around the values of energy that corresponds to $\beta = 0$ or equivalently to the limit $T \rightarrow \infty$, that is precisely the limit where the HTE coefficients A_n are defined, starting with the mean attractive energy,

$$A_1 = \lim_{\beta^* \rightarrow 0} u^*, \quad (13)$$

where $u^* = E/N\epsilon$ and $\beta^* = \epsilon\beta$ are the reduced energy and inverse thermal energy, respectively. The higher-order perturbation terms can be obtained according to the expression

$$A_n = \frac{1}{n!} \lim_{\beta^* \rightarrow 0} \frac{\partial^{(n-1)} u^*}{\partial \beta^{*(n-1)}} \quad (14)$$

III. RESULTS

Computer simulations were performed for SW systems comprised of $N = 512$ particles contained in a unitary box with periodic boundary conditions and reduced densities $\rho^* = \rho\sigma^3$ between 0.1 and 0.7. SW attractive ranges were taken within the interval $1.1 \leq \lambda \leq 1.8$, that are the values required to model real substances, as dos Ramos *et al.* have determined for a wide range of systems in the context of the SAFT-VR approach [28]. Restricting simulations to energy levels where $|\beta^*| \leq 0.1$, the corresponding values of the inverse thermal energy as function of the internal energy u^* were represented by a second-order degree polynomial, for fixed values of ρ^* and λ ,

$$\beta^* = a_0 + a_1 u^* + a_2 u^{*2}. \quad (15)$$

Since the evaluation of the A_n coefficients is performed under the condition of a maximum value of the entropy, or equivalently $\ln \Omega(u^*)$, then a quadratic expression for β^* as a function of u^* is justified due to the gaussian behavior of $\Omega(u^*)$ around $\beta^* = 0$.

In Figure 2 the case $\lambda = 1.5$ is presented for densities $\rho^* = 0.1, 0.4$ and 0.7 from top to bottom. Notice that the mean attractive energy A_1 is given as u^* for $\beta = 0$.

Equation (15) can be easily inverted as

$$u^* = -\frac{a_1 + \sqrt{a_1^2 - 4a_2(a_0 - \beta^*)}}{2a_2}, \quad (16)$$

and from here other thermodynamic properties can be obtained, as the isochoric heat capacity,

$$C_v(u^*) = -\frac{\beta^2}{a_1 + 2a_2 u^*}. \quad (17)$$

Combining Eqs. (14) and (16), the HTE coefficients can be evaluated as function of the fitting parameters a_i

$$A_1 = -\frac{a_1 + \sqrt{a_1^2 - 4a_2 a_0}}{2a_2}, \quad (18a)$$

$$A_2 = -\frac{1}{2\sqrt{a_1^2 - 4a_2 a_0}}, \quad (18b)$$

$$A_3 = \frac{a_2}{3(a_1^2 - 4a_2 a_0)^{3/2}}, \quad (18c)$$

$$A_4 = -\frac{a_2^2}{2(a_1^2 - 4a_2 a_0)^{5/2}}, \quad (18d)$$

$$A_5 = \frac{a_2^3}{(a_1^2 - 4a_2 a_0)^{7/2}}, \quad (18e)$$

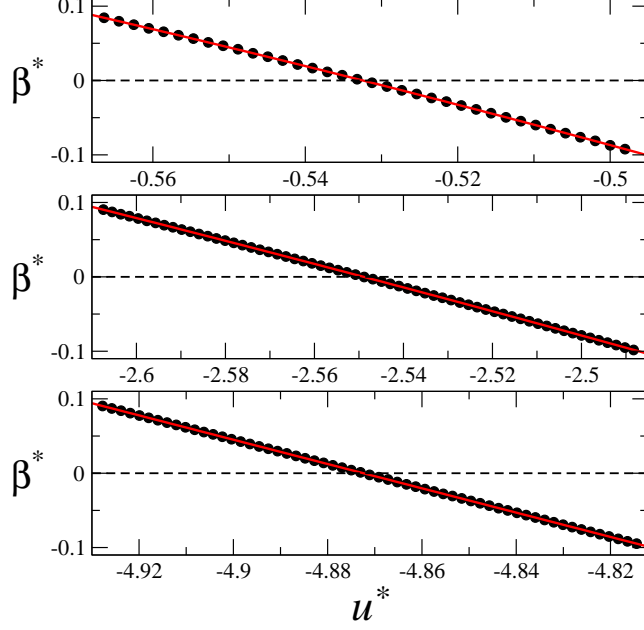


FIG. 2: (Color on line) Inverse temperature as a function of the internal energy u^* for the SW fluid with range $\lambda = 1.5$ and densities $\rho^* = 0.1, 0.4$ and 0.7 , from top to bottom. Black dots denote MCE simulation results and the red solid line is the second-order polynomial fit given in Eq.(15). The value of u^* for $\beta = 0$ corresponds to the first perturbation term A_1 .

$$A_6 = -\frac{7a_2^4}{3(a_1^2 - 4a_2a_0)^{9/2}}, \quad (18f)$$

and so on.

It is useful to realize that the MCE approach offers a simple and straightforward way of extracting information of the perturbation terms by considering β as a function of u^* . From equations (18a)-(18f) we can obtain alternative representations of the perturbation terms,

$$A_2 = \frac{1}{2a_1 + 4a_2A_1}, \quad (19)$$

that corresponds to

$$A_2 = -0.5 \lim_{\beta^* \rightarrow 0} C_v(u^*)/\beta^2, \quad (20)$$

and

$$A_3 = -\frac{a_2}{3}(2A_2)^3, \quad (21)$$

$$A_4 = \frac{a_2^2}{2}(2A_2)^5, \quad (22)$$

$$A_5 = -a_2^3(2A_2)^7, \quad (23)$$

$$A_6 = \frac{7}{3}a_2^4(2A_2)^9. \quad (24)$$

From these expressions, it is clear that the fluctuation terms that are given by the SW perturbation coefficients of order ≥ 2 are basically determined by the high-temperature isochoric heat capacity, C_v , and $a_2 = \partial^2\beta/\partial u^{*2}$. Although previous studies based on the Barker and Henderson perturbation theory modeled A_2 and higher-order terms as functions of the isothermal compressibility approximation [22, 24, 43], *i.e* the fluctuation of the number of hard-spheres particles, the MCE method presented here indicates that it could be more appropriate to use the isochoric heat capacity.

Numerical simulations were implemented with $N \times 10^6$ particle displacement attempts and 30 to 50 different independent runs for every set of parameters. In Fig. 3 results are presented for the first four coefficients and for $\lambda = 1.2$ and $\lambda = 1.5$. NVT MC simulation results for the first three coefficients are also included, these last results were obtained using 864 particles, with 2.5×10^5 cycles required for thermalization and another 5.0×10^5 cycles for averaging. For comparison we include results from Zhou and Solana [51]. In all the cases we observe that the MCE method is in very good agreement with the NVT and external data. Typical values of the absolute average relative deviation between the calculations with MCE and NVT MC methods were 0.11 and 0.04 for the first perturbation term with ranges $\lambda = 1.2$ and $\lambda = 1.5$, respectively. For the cases for A_2 and A_3 these values increase for the same systems: 0.17 and 0.12 for A_2 , 8.6 and 19.3 for A_3 , for $\lambda = 1.2$ and $\lambda = 1.5$, respectively.

The HTE coefficients, up to A_6 are listed in Table I for all the SW ranges λ considered in this work.

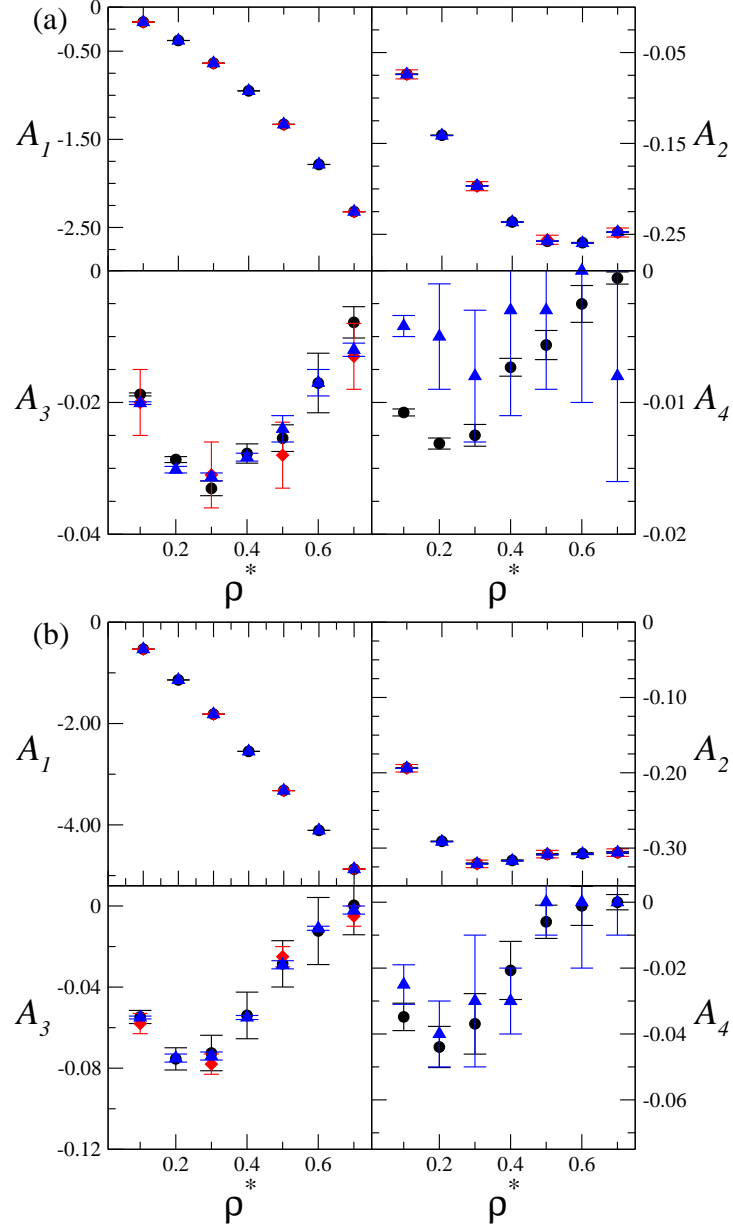


FIG. 3: (Color on line) First HTE coefficients A_n for (a) $\lambda = 1.2$ and (b) $\lambda = 1.5$ as function of ρ^* . Black circles are results obtained with Equations (18), red diamonds are NVT-MC simulations and blue triangles are values taken from Ref. [51].

TABLE I: HTE Coefficients for all λ ranges up to A_6 .

ρ^*	A_1	A_2	A_3	A_4	A_5	A_6
$\lambda = 1.1$						
0.10	-0.07753(97)	-0.0359(21)	-0.0087(22)	-0.0047(26)	-0.0034(29)	-0.0029(33)
0.20	-0.17686(98)	-0.0762(26)	-0.019(13)	-0.010(15)	-0.008(17)	-0.007(20)
0.30	-0.3036(11)	-0.1189(32)	-0.025(29)	-0.012(30)	-0.008(32)	-0.006(37)
0.40	-0.4652(13)	-0.1624(62)	-0.027(43)	-0.010(33)	-0.005(25)	-0.003(21)
0.50	-0.6715(16)	-0.2045(92)	-0.027(92)	-0.008(61)	-0.003(45)	-0.001(37)
0.60	-0.9350(18)	-0.241(11)	-0.02(13)	-0.005(66)	-0.001(43)	-0.000(33)
0.70	-1.270(13)	-0.269(12)	-0.01(13)	-0.001(40)	-0.000(19)	-0.000(11)
$\lambda = 1.2$						
0.10	-0.16893(82)	-0.0737(25)	-0.019(11)	-0.011(12)	-0.008(14)	-0.007(17)
0.20	-0.37858(75)	-0.1409(29)	-0.029(22)	-0.013(20)	-0.008(19)	-0.006(18)
0.30	-0.6361(12)	-0.1966(55)	-0.033(56)	-0.012(42)	-0.006(32)	-0.004(27)
0.40	-0.9503(11)	-0.2364(61)	-0.028(74)	-0.007(34)	-0.003(18)	-0.001(10)
0.50	-1.3305(17)	-0.2576(86)	-0.02(11)	-0.005(53)	-0.001(33)	-0.000(25)
0.60	-1.7851(20)	-0.259(15)	-0.02(22)	-0.003(66)	-0.001(42)	-0.000(28)
0.70	-2.3203(17)	-0.248(12)	-0.00(11)	-0.000(21)	-0.0001(71)	-0.0000(27)
$\lambda = 1.3$						
0.10	-0.27460(90)	-0.1125(37)	-0.030(28)	-0.018(33)	-0.014(40)	-0.013(51)
0.20	-0.60525(75)	-0.1964(40)	-0.039(48)	-0.017(43)	-0.010(40)	-0.007(39)
0.30	-0.99738(84)	-0.2482(54)	-0.041(37)	-0.015(28)	-0.008(21)	-0.004(16)
0.40	-1.4563(15)	-0.2695(76)	-0.036(77)	-0.011(44)	-0.004(27)	-0.002(18)
0.50	-1.9842(18)	-0.267(10)	-0.033(50)	-0.009(28)	-0.003(16)	-0.0014(99)
0.60	-2.5782(20)	-0.255(16)	-0.02(11)	-0.004(54)	-0.001(33)	-0.000(23)
0.70	-3.2283(80)	-0.245(12)	0.012(78)	-0.001(19)	-0.0002(60)	-0.0000(22)
$\lambda = 1.4$						
0.10	-0.39549(77)	-0.1527(41)	-0.040(36)	-0.023(43)	-0.018(51)	-0.017(63)
0.20	-0.85818(84)	-0.2454(52)	-0.053(30)	-0.026(30)	-0.017(29)	-0.013(30)
0.30	-1.3894(11)	-0.2864(60)	-0.055(68)	-0.023(59)	-0.013(51)	-0.009(47)
0.40	-1.9871(17)	-0.292(18)	-0.05(13)	-0.017(90)	-0.008(66)	-0.005(53)
0.50	-2.6437(26)	-0.283(17)	-0.03(18)	-0.01(11)	-0.003(87)	-0.001(79)
0.60	-3.3432(49)	-0.279(37)	-0.02(26)	-0.002(93)	-0.000(65)	-0.000(48)
0.70	-4.0611(25)	-0.278(10)	0.01(11)	-0.001(20)	-0.0001(64)	-0.000(23)
$\lambda = 1.5$						
0.10	-0.53247(43)	-0.1936(22)	-0.055(32)	-0.035(42)	-0.030(54)	-0.029(73)
0.20	-1.13921(70)	-0.2910(41)	-0.075(55)	-0.044(62)	-0.034(72)	-0.031(86)
0.30	-1.8150(12)	-0.3204(71)	-0.073(87)	-0.037(92)	-0.025(98)	-0.02(11)
0.40	-2.5489(15)	-0.3164(92)	-0.05(11)	-0.020(88)	-0.010(72)	-0.006(64)
0.50	-3.3224(16)	-0.308(10)	-0.03(12)	-0.006(53)	-0.002(28)	-0.000(17)
0.60	-4.1085(21)	-0.307(12)	-0.01(18)	-0.001(55)	-0.000(37)	-0.000(32)
0.70	-4.8724(23)	-0.306(13)	0.00(14)	-0.000(24)	-0.0000(84)	-0.0000(29)
$\lambda = 1.6$						
0.10	-0.68671(81)	-0.2368(52)	-0.073(52)	-0.051(74)	-0.05(10)	-0.05(15)
0.20	-1.4506(11)	-0.3356(59)	-0.101(53)	-0.068(72)	-0.061(98)	-0.06(14)
0.30	-2.2786(14)	-0.3550(75)	-0.087(99)	-0.05(11)	-0.04(12)	-0.03(15)
0.40	-3.1503(14)	-0.3468(93)	-0.054(94)	-0.019(68)	-0.009(51)	-0.005(40)
0.50	-4.0379(20)	-0.342(14)	-0.02(12)	-0.002(35)	-0.000(13)	-0.0001(54)
0.60	-4.9063(25)	-0.340(12)	0.00(12)	-0.000(14)	0.0000(39)	-0.00000(99)
0.70	-5.7174(26)	-0.331(14)	0.01(12)	-0.000(16)	0.0000(45)	-0.0000(12)
$\lambda = 1.7$						
0.10	-0.85948(87)	-0.2828(56)	-0.098(59)	-0.077(94)	-0.08(15)	-0.10(25)
0.20	-1.7953(11)	-0.3821(86)	-0.131(63)	-0.100(96)	-0.10(15)	-0.12(23)
0.30	-2.7860(11)	-0.3930(95)	-0.099(74)	-0.056(85)	-0.042(99)	-0.04(12)
0.40	-3.8031(19)	-0.383(10)	-0.04(12)	-0.011(60)	-0.004(33)	-0.001(20)
0.50	-4.8118(21)	-0.379(14)	-0.00(13)	-0.000(13)	-0.000(03)	-0.00000(85)
0.60	-5.7751(24)	-0.378(15)	-0.01(20)	-0.000(31)	0.000(12)	-0.0000(45)
0.70	-6.6587(35)	-0.375(16)	0.01(17)	-0.001(26)	0.0001(91)	-0.0000(33)
$\lambda = 1.8$						
0.10	-1.0522(11)	-0.3320(50)	-0.130(36)	-0.114(64)	-0.13(11)	-0.18(21)
0.20	-2.1769(11)	-0.4316(76)	-0.170(81)	-0.15(14)	-0.18(25)	-0.24(47)
0.30	-3.3452(10)	-0.436(11)	-0.117(86)	-0.07(10)	-0.06(13)	-0.05(16)
0.40	-4.5225(15)	-0.425(12)	-0.05(11)	-0.012(53)	-0.004(27)	-0.002(15)
0.50	-5.6725(26)	-0.422(13)	-0.01(17)	-0.000(18)	-0.0000(47)	-0.0000(11)
0.60	-6.7632(25)	-0.426(14)	0.00(18)	-0.000(31)	0.000(12)	-0.0000(48)
0.70	-7.7753(32)	-0.437(18)	-0.01(16)	-0.000(20)	-0.0000(52)	-0.0000(14)

A. Thermodynamic of SW fluids

The MCE results for the HTE coefficients are required to generate the equation of state for the monomeric SW fluid as well as for SW chain molecules in the context of the SAFT-VR approach [25]. In this section we describe simple functional expressions to represent the MCE values, obtained by fitting appropriate analytical expressions to the simulated values of the coefficients.

For A_1 the data can be represented by a third order polynomial without an independent term

$$A_1(\rho^*) = b_0\rho^* + b_1\rho^{*2} + b_2\rho^{*3}, \quad (25)$$

whereas A_2 can be approximated by

$$A_2(\rho^*) = g_2\rho^* e^{-h_2\rho^{*2}} + f_2 \tanh(c_2\rho^*), \quad (26)$$

except for $\lambda = 1.1$, where the relation is the same that the one for A_1 . In the same way, similar expressions can be found for the higher-order coefficients,

$$A_i(\rho^*) = g_i\rho^* e^{-h_i\rho^{*2}}, \quad \text{for } i \geq 3. \quad (27)$$

In Figure 4 results are given for the first six perturbation terms as obtained from MCE simulations and parametrical representation. The summary of the fitting parameters are listed in Tables II-IV.

TABLE II: Fitting parameters with Eq. (25).

λ	b_0	b_1	b_2
1.10	-0.74484	-0.382173	-1.63313
1.20	-1.51817	-1.58568	-1.40168
1.30	-2.40494	-3.04343	-0.16285
1.40	-3.46854	-4.36238	1.46006
1.50	-4.74229	-5.34853	3.10155
1.60	-6.24987	-5.88535	4.48369
1.70	-8.01193	-5.8906	5.34814
1.80	-10.0523	-5.27555	5.38749

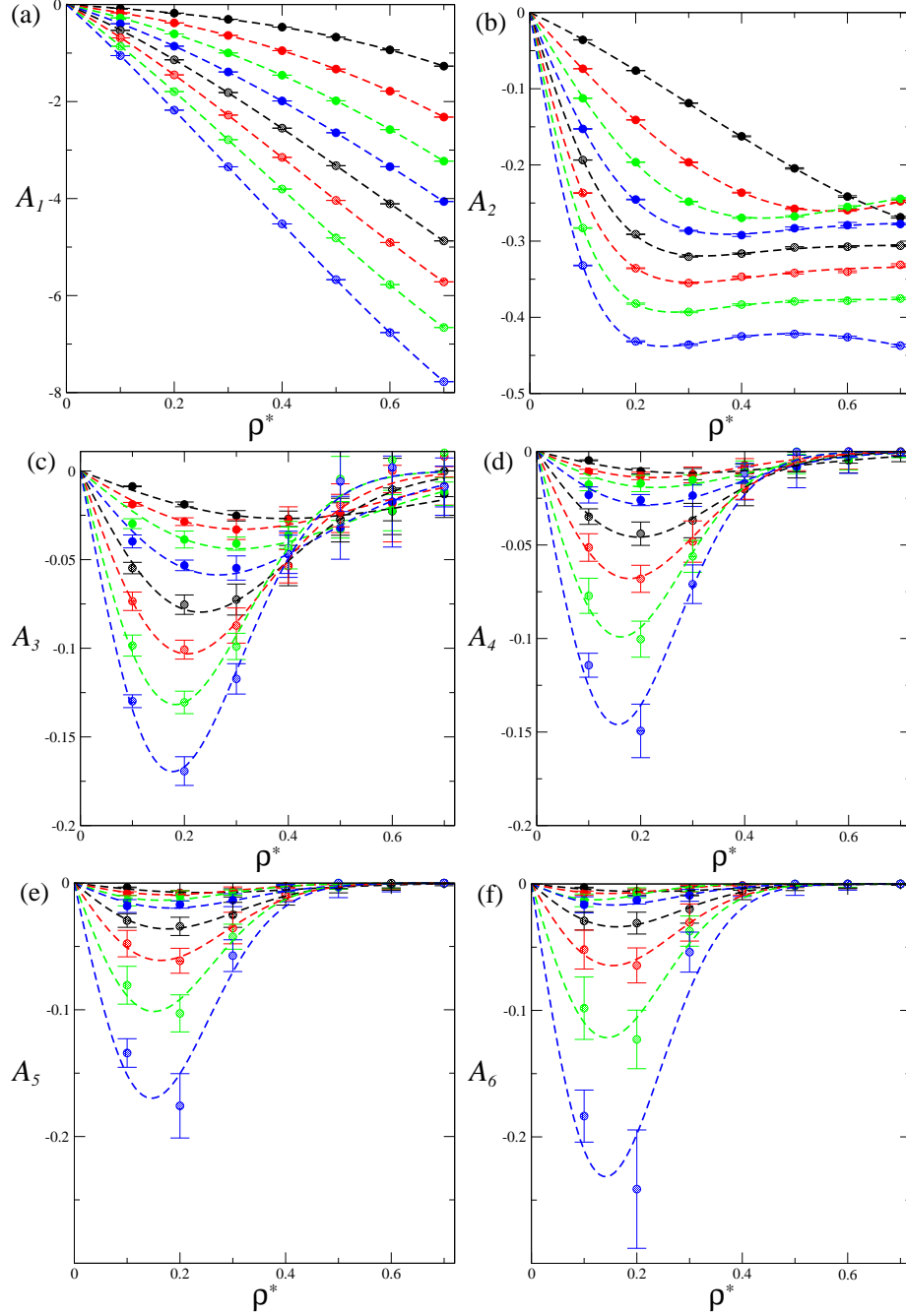


FIG. 4: (Color on line) HTE coefficients A_n for SW ranges λ considered in this work as function of ρ^* for (a) A_1 , (b) A_2 , (c) A_3 , (d) A_4 , (e) A_5 and (f) A_5 . In all the cases the MCE simulations are depicted as solid circles and the dashed lines represent the fitted data according to relations (25), (26) and (27).

With the expressions given for the perturbation terms, and using the Carnahan-Starling equation of state for the HS reference system, i.e.,

$$\frac{A_0^E}{NkT} = \frac{4\eta^2 - 3\eta}{(1 - \eta)^2}, \quad (28)$$

where $\eta = \pi\rho\sigma^3/6$ is the packing fraction of the fluid, then it is possible to predict the phase behavior of the SW fluid. For example, in Figure 5 we present results for the liquid-vapor equilibria obtained when perturbation terms are added sequentially. Results are compared with Gibbs-Ensemble MC simulations [21]. We can observe that the higher the order of the perturbation term included, the lower the critical point obtained. However, it seems that the behavior of the coexistence curves is very sensitive to the parametrization proposed for A_5 and A_6 , and that using the equation of state up to fourth order gives the best representation of the shape of this curve. Since the proper modeling of the coexistence zone near the critical region requires to include more robust approaches based on the renormalization method, as discussed previously for the SAFT-VR method [70, 71], we can expect that the MCE-SW thermodynamic modeling could also be combined with those approaches in order to give a more accurate prediction of the critical properties of SW fluids.

TABLE III: Fitting parameters with Eq. (26) for $\lambda \geq 1.2$. For $\lambda = 1.1$ the data are fitted with $A_2 = -0.315714\rho^* - 0.405783\rho^{*2} + 0.4394\rho^{*3}$.

λ	g_2	h_2	f_2	c_2
1.20	-0.754123	1.54113	0.00000	0.00000
1.30	-0.400299	4.81518	-0.221092	3.42486
1.40	-0.311957	9.62637	-0.275382	4.80383
1.50	-0.301985	12.7536	-0.305239	6.10676
1.60	-0.242938	10.8684	-0.333435	7.67705
1.70	-0.310091	16.5368	-0.376464	8.31355
1.80	-0.385677	1.98941	0.539128	8.40071

The convergence rate of the MCE perturbation terms can also be determined through the isochoric heat capacity, as shown in Figure 6 for a SW fluid with range $\lambda = 1.5$ and reduced temperature $T^* = 1.5$. When compared with the MCE simulated values for the non-perturbed system [64], the corresponding approximation obtained through the MCE

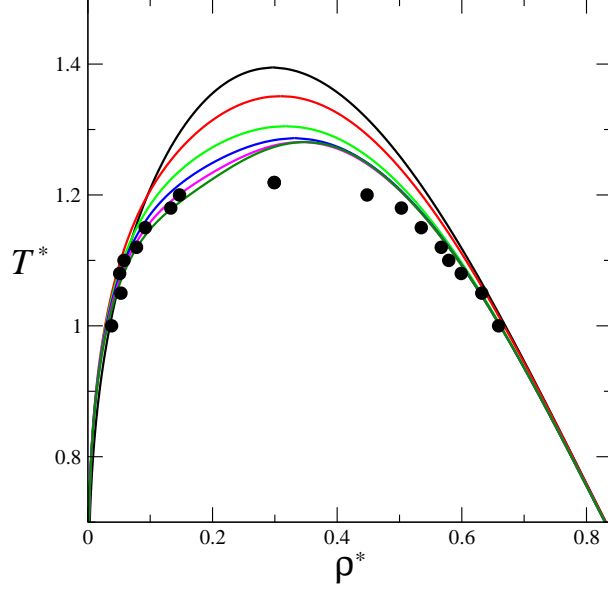


FIG. 5: (Color online) Liquid-vapor equilibria for the SW fluid of range $\lambda = 1.5$ using sequential perturbation terms from A_1 up to A_6 . Gibbs Ensemble Monte Carlo computer simulations [21] are included for comparison.

perturbation terms indicates that the expansion up to sixth order gives an accurate prediction of the non-perturbed value. In the same figure we report the predictions obtained from Eqs. (25)-(27), that clearly are very accurate.

TABLE IV: Fitting parameters with Eq. (27) for $i > 2$.

λ	g_3	h_3	g_4	h_4	g_5	h_5	g_6	h_6
1.10	-0.112095	3.21962	-0.0649142	5.84165	-0.0504391	8.30714	-0.0456578	10.5817
1.20	-0.175887	5.26299	-0.103055	10.0468	-0.085633	16.1883	-0.0847178	23.5119
1.30	-0.239451	5.46669	-0.139246	9.65685	-0.136693	18.7422	-0.170437	34.0676
1.40	-0.364466	7.11089	-0.218461	10.8009	-0.177024	14.9085	-0.175455	20.3773
1.50	-0.568689	9.38497	-0.385468	13.0504	-0.338921	16.1663	-0.345938	19.133
1.60	-0.828532	11.8677	-0.627884	15.717	-0.615139	18.6941	-0.69147	21.1024
1.70	-1.18847	14.9645	-1.01203	19.1651	-1.11077	22.1139	-1.39728	24.2925
1.80	-1.57846	15.9349	-1.54308	20.5372	-1.91277	23.335	-2.70865	25.1763

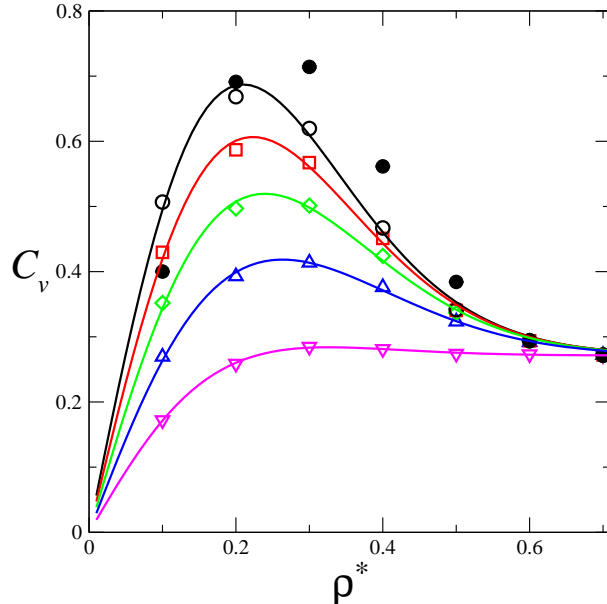


FIG. 6: (Color online) Contributions to the SW fluid isochoric heat capacity for $\lambda = 1.5$ and $T^* = 1.5$ using MCE simulated values from A_2 (purple triangles) up to A_6 (open circles). Solid black symbols denote the non-perturbative MCE computer simulation values. The lines correspond to the predictions given by equations (25)-(27)

IV. CONCLUSIONS

We have implemented a new protocol based on the MCE method for the evaluation of the HTE perturbation terms of the SW fluid. This method has the advantage of allowing the evaluation with great accuracy of higher order coefficients in the high-temperature expansion for discrete-potential systems. Expressions for these terms have been obtained, either in parametric form as parabolic coefficients of fittings to the MCE simulated values, or as analytical functions on density and temperature that reproduce these values, that are used to determine the equation of state of the system. An interesting result that comes out from the MCE approach is that the SW perturbation terms of order higher than 1 can be expressed in terms of the high-temperature value of the isochoric heat capacity, instead of the HS isothermal compressibility as occurs in the NVT modeling, suggesting an alternative route to model the equation of state for SW fluids. Results have been presented for the SW liquid-vapor coexistence curve and for the isochoric heat capacity. In both cases the convergence of the perturbation expansion has been determined from the MCE simulated

values.

The MCE is a promising approach that could help to have a better understanding of the role of higher-order perturbation terms in equations of state used to study the phase diagram of molecular fluids, following the same lines of research presented by Westen and Gross [72] recently developed for the HTE modeling of continuous-potential systems such as the Lennard-Jones fluid.

Acknowledgments

FS acknowledges the support by Universidad de Guanajuato (México) Proyecto DAIP 879/2016.

-
- [1] P. T. Cummings and G. Stell, *Mol. Phys.* **51**, 253 (1984).
- [2] G. A. Chapela, L. E. Scriven and H. T. Davies, *J. Chem. Phys.* **91**, 4307 (1989).
- [3] A. L. Benavides and A. Gil-Villegas, *Mol. Phys.* **97**, 1225 (1999).
- [4] A. Vidales, A. L. Benavides and A. Gil-Villegas, *Mol. Phys.* **99**, 703 (2001).
- [5] J. R. Elliott, Jr, *Fluid Phase Eq.* **194**, 161 (2002).
- [6] J. Cui and J. R. Elliott, Jr, *J. Chem. Phys.* **116**, 8625 (2002).
- [7] S. J. Mejía-Rosales, A. Gil-Villegas, B. I. Ivlev and J. Ruíz-García, *J. Phys.: Condens. Matter* **14**, 4795 (2002).
- [8] S. J. Mejía-Rosales, A. Gil-Villegas, B. I. Ivlev and J. Ruíz-García, *J. Phys. Chem. B* **110**, 22230 (2006).
- [9] A. L. Benavides, L. A. del Pino, A. Gil-Villegas and F. Sastre, *J. Chem. Phys.* **125**, 204715 (2006).
- [10] J. Torres-Arenas, L. A. Cervantes, A. L. Benavides, G. A. Chapela and F. del Río, *J. Chem. Phys.* **132**, 034501 (2010).
- [11] G. A. Chapela, F. del Río, A. L. Benavides and J. Alejandre, *J. Chem. Phys.* **133**, 234107 (2010).
- [12] F. A. Perdomo and A. Gil-Villegas, *Fluid Phase Eq.* **293**, 182 (2010).
- [13] F. A. Perdomo and A. Gil-Villegas, *Fluid Phase Eq.* **306**, 124 (2011).
- [14] F. del Río and A. Gil-Villegas, *J. Phys. Chem.* **95**, 787 (1991).
- [15] M. Castro, J. L. Mendoza de la Cruz, E. Buenrostro-González, S. López-Ramírez and A. Gil-Villegas, *Fluid Phase Eq.* **286**, 113 (2009).
- [16] G. Jiménez-Serratos, S. Santillán, C. Avendano, M. Castro and A. Gil-Villegas, *Oil and Gas Sci. Tech.* **63**, 329 (2008).
- [17] V. M. Trejos, M. Becerra, S. Figueroa-Gerstenmaier and A. Gil-Villegas, *Mol. Phys.* **112**, 2330 (2014).
- [18] A. Martínez, V. M. Trejos and A. Gil-Villegas, *Fluid Phase Eq.* *in press* (2017).
- [19] M. H. J. Hagen and D. Frenkel, *J. Chem. Phys.* **101** 4093 (1994).
- [20] W. C. K. Poon and P. N. Pusey *Observation, Prediction and Simulation of Phase Transition in Complex Fluids*, NATO ASI series C, Vol 460 (1995).

- [21] L. Vega, E. de Miguel, L. F. Rull, G. Jackson, and I. A. McLure, *J. Chem. Phys.* **96**, 2296 (1992).
- [22] A. Gil-Villegas and F. del Río, *Rev. Mex. Fis.* **39**, 526 (1993).
- [23] J. Chang and S. I. Sandler, *Mol. Phys.* **81**, 745 (1994).
- [24] A. Gil-Villegas, F. del Río and A. L. Benavides, *Fluid Phase Eq.* **119**, 97 (1996).
- [25] A. Gil-Villegas, A. Galindo, P. J. Whitehead, S. Mills, G. Jackson and A. Burgess, *J. Chem. Phys.* **106**, 4168 (1997).
- [26] A. Galindo, L. A. Davies, A. Gil-Villegas and G. Jackson, *Mol. Phys.* **93**, 241 (1998).
- [27] B. H. Patel, H. Docherty, S. Varga, A. Galindo and G. C. Maitland, *Mol. Phys.* **103**, 129 (2005).
- [28] M. C. dos Ramos, H. Docherty, F. J. Blas and A. Galindo, *Fluid Phase Eq.* **276**, 116 (2009).
- [29] J. Cui and J. R. Elliott, Jr, *J. Chem. Phys.* **114**, 7283 (2001).
- [30] F. del Río, E. Ávalos, R. Espíndola-Heredia, L. F. Rull, G. Jackson and S. Lago, *Mol. Phys.* **100**, 2531 (2002).
- [31] E. Schöll-Paschinger, A. L. Benavides and R. Castañeda-Priego, *J. Chem. Phys.* **123**, 234513 (2005).
- [32] A. L. Benavides, Y. Guevara and F. del Río, *Phys. A* **202**, 420 (1994).
- [33] F. del Río, A. L. Benavides and Y. Guevara, *Phys. A* **215**, 10 (1995).
- [34] Y. Guevara, A. L. Benavides, A. F. Estrada-Alexanders and M. Romero, *J. Phys. Chem. B* **104**, 7490 (2000).
- [35] A. L. Benavides and Y. Guevara, *J. Phys. Chem. B* **107**, 9477 (2003).
- [36] A. L. Benavides and F. Gamez, *J. Chem. Phys.* **135**, 134511 (2011).
- [37] W. R. Smith, D. Henderson, and J. A. Barker, *J. Chem. Phys.* **53**, 508 (1970).
- [38] B. J. Alder, D. A. Young and M. A. Mark, *J. Chem. Phys.* **56**, 3013 (1972).
- [39] D. Henderson, W. G. Madden, and D. D. Fitts, *J. Chem. Phys.* **64**, 5026 (1976).
- [40] D. Henderson, O. Scalise and W. R. Smith, *J. Chem. Phys.* **72**, 2431 (1980).
- [41] K. H. Lee, M. Lombardo and S. I. Sandler, *Fluid Phase Eq.* **2**, 177 (1985).
- [42] P. D. Fleming and R. J. Brugman, *AIChE J.* **33**, 729 (1987).
- [43] A. L. Benavides and F. del Río, *Mol. Phys.* **68**, 983 (1989).
- [44] D. A. de Lonngi, P. A. Longgi and J. Alexandre, *Mol. Phys.* **71**, 427 (1990).
- [45] Y. Tang and B. C.-Y. Lu, *J. Chem. Phys.* **100**, 6665 (1994).

- [46] S. B. Yuste and A. Santos, *J. Chem. Phys.* **101**, 2355 (1994).
- [47] A. Gil-Villegas, C. Vega, F. del Río and A. Malijevský, *Mol. Phys.* **86**, 857 (1995).
- [48] J. Largo and J. R. Solana, *Fluid Phase Equilib.* **193**, 277 (2002).
- [49] J. Largo, J. R. Solana, L. Acedo and A. Santos, *Mol. Phys* **101**, 2981 (2003).
- [50] R. Espíndola-Heredia, F. del Río and A. Malijevský, *J. Chem. Phys.* **130**, 024509 (2009).
- [51] S. Zhou and J. R. Solana, *J. Chem. Phys.* **138**, 244115 (2013).
- [52] C. McCabe, A. Gil-Villegas, G. Jackson and F. del Río, *Mol. Phys.* **97**, 551 (1999).
- [53] A. Martínez, M. Castro, C. McCabe and A. Gil-Villegas, *J. Chem. Phys.* **126**, 074707 (2007).
- [54] G. Jiménez-Serratos, A. Gil-Villegas, C. Vega and F. J. Blas, *J. Chem. Phys.* **139**, 114901 (2013).
- [55] D. C. Williamson and Y. Guevara, *J. Phys. Chem. B* **103**, 7522 (1999).
- [56] D. C. Williamson and F. del Río, *J. Chem. Phys.* **109**, 4675 (1996).
- [57] E. García-Sánchez, A. Martínez-Richa, J. A. Villegas-Gasca, L. H. Mendoza-Huizar and A. Gil-Villegas, *J. Phys. Chem. A* **106**, 10342 (2002).
- [58] B. Martínez-Haya, L. F. Rull, A. Cuetos and S. Lago, *Mol. Phys.* **99**, 509 (2001).
- [59] B. Martínez-Haya, A. Cuetos and S. Lago, *Phys. Rev. E* **67**, 051201 (2003).
- [60] L. Wu, E. A. Müller and G. Jackson, *Macromolecules* **47**, 1482 (2014).
- [61] V. M. Trejos and A. Gil-Villegas, *J. Chem. Phys.* **136**, 184506 (2012).
- [62] C. Serna and A. Gil-Villegas, *Mol. Phys.* **114**, 2700 (2016).
- [63] R. W. Zwanzig, *J. Chem. Phys.* **22**, 1420 (1954).
- [64] F. Sastre, A. L. Benavides, J. Torres and A. Gil-Villegas, *Phys. Rev E* **92**, 033303 (2015)
- [65] A. Hüller and M. Pleimling, *Int. Journal of Modern Physics C*, **13**, 947 (2002).
- [66] P. M. C. de Oliveira, T. J. P. Penna and H. J. Herrmann, *Braz. J. Phys.* **26**, 677 (1996).
- [67] P. M. C. de Oliveira, T. J. P. Penna and H. J. Herrmann, *Eur. Phys. J. B* **1**, 205 (1998).
- [68] P. M. C. Oliveira, *Eur. Phys. J.* **B6**, 111 (1998).
- [69] M. Kastner, M. Promberger and J. D. Muñoz, *Phys. Rev. E* **62**, 7422 (2000).
- [70] C. McCabe and S. B. Kiselev, *Fluid Phase Eq.* **219**, 3 (2004).
- [71] E. Forte, F. Llovel, L. F. Vega, J. P. M. Trusler and A. Galindo, *J. Chem. Phys.* **134**, 154102 (2011).
- [72] T. van Westen and Joachim Gross, *J. Chem. Phys.* **147**, 014503 (2017).